Asian Journal of Chemistry; Vol. 32, No. 12 (2020), 2991-2996

ASIAN JOURNAL OF CHEMISTRY

https://doi.org/10.14233/ajchem.2020.22828

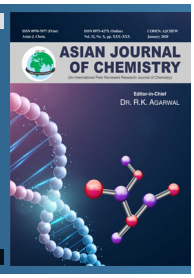

Spectral Characterization, Antioxidant, Cytotoxic and Molecular Docking Studies of Nanosized Cu(II) Hybrid with 2-Hydroxyphenylethylideneamino)quinolin-2(1*H*)-one

MUREFAH M. ANAZY[1], AMANI S. ALTURIQI[1], EIDA S. AL-FARRAJ[2] and REDA A. AMMAR[3,*]

[1]Department of Chemistry, College of Science, Princess Nourah Bint Abdulrahman University, Riyadh, Saudi Arabia
[2]Department of Chemistry, College of Science, Imam Mohammad Ibn Saud Islamic University (IMSIU), 13623, Riyadh, Saudi Arabia
[3]Department of Chemistry, College of Science, Al Azhar University, Cairo, Egypt

*Corresponding author: E-mail: dr_reda06@yahoo.com

Received: 3 July 2020; *Accepted*: 12 August 2020; *Published online*: 7 December 2020; AJC-20128

Nanosized Cu(II) hybrids derived 2-hydroxyphenylethylideneamino)quinolin-2(1*H*)-one (HPEAQ) was synthesized and characterized by spectroscopic and TGA analysis. The IR, ^{1}H & ^{13}C NMR spectra revealed that the HPEAQ coordinated its CH=N, C=O and deprotonated hydroxyl groups in coordination with Cu(II) ions (**1-4**). The geometries of copper(II) hybrids are octahedral geometry. The XRD and SEM images unequivocally definite the nanosized copper chelate (2). The antioxidant, cytotoxic activities and molecular docking technique of the compounds have also been screened.

Keywords: Nanosized Cu(II) hybrid, 2-Hydroxyphenylethylideneamino)quinolin-2(1*H*)-one, Antioxidant activity, Cytotoxic activity.

INTRODUCTION

Schiff-base ligands played a substantial role in the enhancement of current coordination chemistry due to their relevance to numerous multi-faceted research field [1-8]. They form a crucial class of the most commonly employed organic compounds and present many applications in numerous fields such as oxidation catalysts, hydrogenation, industrial dyes and reagent for analysis [9-11]. The N,O,S-containing hetero-cyclic Schiff bases present various pharmacological activities, including antibacterial, antimicrobial, antioxidant, antifungal, and anticancer [12-17]. Schiff base complexes are among the most crucial models of stereochemistry in *d-d* transition coordination chemistry and essential groups due to their selectivity, synthetic flexibility, and sensibility in metallic ions [18]. They have excellent properties, including antifungal, antibacterial, antiviral, antitumor, anti-inflammatory and cytotoxic activities [19]. Schiff base complexes also have diversified biological, clinical, and pharmacological applications, and various derivatives of these complexes are used as medicines [20,21].

The compositions of covalent organic substructures of azomethine Schiff base have been investigated through the covalent molecular assembly of Schiff base interactions along with layer-by-layer processes [22]. These substructures include porous crystalline structures with three or two dimensions. Most of the azomethine Schiff bases have an interesting mechanism for chelation with metallic ions to produce the corresponding coordination compounds of the *d-d* transitions, main group, actinides and lanthanides having evidently enhanced properties due to chelation with metal (I/II/III/IV) ions [23]. This phenomenon can occur because their elastic and stereoelectronic structures lead to the formation of varieties of coordination compounds having various applications, such as clandestine fluid flow tracking [24] and medicinal and bio-inorganic chemistry [25,26]. The derivatives of metal(III) azomethine Schiff base of equatorial tetradentate ligand *bis*(acetylacetone)-ethylenediimine (A), $[Co(A)L_2]^+$ (L = NH_3, imidazoles) inhibit the histidine containing protein by dissociatively exchanging labile-axial chelating agents [27-29]. Azomethine Schiff bases metal complexes exhibit non-linear optical, fluorescence, and DNA-binding properties [30-32]. These derivatives are also employed as components of pharmaceutically active cocrystals and in polymeric materials, sensors, energy materials, nuclear medicine and organic photovoltaic materials [33-35]. In this work, a new Schiff base derived through the condensation of 1-aminoquinolin-2(1*H*)-one with 1-(2-hydroxyphenyl) ethan-1-one is synthesized. Further, divalent transition metal complexes with the newly synthesized ligand were also synthesized

and characterized using FT-IR, ultraviolet visible, ^{1}H, ^{13}C and ^{15}N NMR spectroscopic techniques. After complete theoretical and experimental structural analyses, against a standard reference compound, we examined the antimicrobial activities of the novel [Cu(HPEAQ)(H_2O)$_2$] complex (HPEAQ = 2-(hydroxyphenylethylideneamino)quinolin-2(1*H*)-one). The cytotoxicity of [Cu(HPEAQ)(H_2O)$_2$] was determined against 5-fluorouracil (5-FU) breast cancer and Hep-G2 liver carcinoma cell lines. The evaluation of biological activities and molecular docking were employed to support the results.

EXPERIMENTAL

The magnetic susceptibilities were determined using Sherwood balance at room temperature.Electronic spectra were conducted on a Unicam UV-vis spectrophotometer. The IR spectra were obtained on a Mattson 5000 FTIR spectrophotometer in a solid state, while ^{1}H NMR spectra were obtained from Perkin-Elmer 300 MHz spectrometer. A Perkin-Elmer CHN Analyzer 2400 was used to estimate elemental analysis with deuterated organic solvents and TWS being utilized as an internal standard. A Jeol-300 MHz EPR spectrometer was employed to estimate the copper complex values from the electron paramagnetic resonance spectrum. Furthermore, TGA and DTA (20-1000 ºC) were obtained at a nitrogen flow rate under 20 mL/min and a heating rate of 15 ºC/min on a DTG-50 Shimadzu analyzer.

Synthesis of 2-(hydroxy-phenylethylideneamino)quinolin-2(1*H*)-one) (HPEAQ): The ligand HPEAQ was synthesized by dissolving 1-(2-hydroxyphenyl)ethan-1-one (0.005 M) and 1-aminoquinolin-2(1*H*)-one (0.005 M, 15 mL dissovled in ethanol). The mixture was refluxed in a water bath for 3 h. The product was washed with absolute ethanol and evaporated to dryness (**Scheme-I**). Colour: orange; yield: 88%; Elemental analysis; calcd. (found) %: C, 72.72 (72.63); H, 4.58 (4.49); N, 10.60 (10.54).

Synthesis of Cu(II) hybrids

Reflux conditions: The Cu(II) hybrid **(1)** was obtained by mixing 0.01 M of $CuCl_2{\cdot}2H_2O$ with 0.01 M of HPEAQ in ethanol (30 mL). The mixture was refluxed at 60 ºC for 5 h. The solid hybrid was filtered then washed, recrystallized and dried in a vacuum. Yield: 47 %; pale brown; Elemental analysis calcd. (found) % for $C_{16}H_{15}ClCuN_2O_4$: C, 48.25 (48.18); H, 3.80 (3.74); Cl, 8.90 (8.83); Cu, 15.95 (15.90); N, 7.03 (6.97).

Hydrothermal conditions: Copper salt ($CuCl_2{\cdot}2H_2O$, 0.1 mmol) and the synthesized azomethine Schiff base ligand HPEAQ were dissolved in 50 mL of water, stirred for 15 min and then transferred into a Teflon-lined stainless steel autoclave. After treatment at different temperatures *viz*. 120, 140 and 160 ºC). The products were washed with distilled water and dried under vacuum.

At 120 ºC (2): Yield: 73%; colour: brown; Elemental analysis calcd. (found) % for $C_{16}H_{15}N_2O_4ClCu$: C, 48.25 (48.14); H, 3.80 (3.72); Cl, 8.90 (8.81); Cu, 15.95 (15.89); N, 7.03 (6.94).

At 140 ºC (3): Yield: 69%; colour: brown; Elemental analysis calcd. (found) % for $C_{16}H_{15}N_2O_4ClCu$: C, 48.25 (48.22); H, 3.80 (3.74); Cl, 8.90 (8.87); Cu, 15.95 (15.90); N, 7.03 (6.93).

At 160 ºC (4): Yield: 64%; colour: Amber; Elemental analysis calcd. (found) % for $C_{16}H_{15}N_2O_4ClCu$: C, 48.25 (48.21); H, 3.80 (3.78); Cl, 8.90 (8.88); Cu, 15.95 (15.91); N, 7.03 (6.99).

Antioxidant activity: The erythrocyte hemolysis, ABTS, and DPPH of the antioxidant activity were determined [36-38] using eqn. 1, where the free radical ABTS and DPPH percentage of inhibition (I%) was measured.

$$I\ (\%) = \frac{\text{Absorbance of sample}}{\text{Absorbance of blank}} \times 100$$

Cytotoxic activity: For cytotoxic activity, the cell viability and Ehrlich ascites were estimated microscopically through examination [39,40].

RESULTS AND DISCUSSION

Copper(II) hybrids having nanosize were acquired using the refluxing method and also by hydrothermally treating the synthesized azomethine Schiff base ligand (HPEAQ) with copper(II) metal salt in a ratio of 1:1 at different temperatures *viz*. 120, 140 and 160 ºC. The data of the elemental analysis of nanosized hybrids were in strong agreement with hybrids obtained under the reflux condition.

Characterization of azomethine Schiff base ligand (HPEAQ): The ^{1}H NMR signals of the aromatic, OH, CH_3, CH and CH=N proton appeared at δ 6.72-8.13, 11.08, 4.3, 4.1 and 8.27 ppm, respectively. The ^{13}C NMR spectrum signals appeared at δ 64, 52, 117-133, 164, 142 and 168 ppm indicated the existence of CH, CH_3, phenyl, C–OH, CH=N and C=O carbon, respectively. In the ^{15}N NMR spectrum, the signals of N_1 (quinoline) and N_{12} (azomethine) were appeared at 164.2 and 245.3 ppm, respectively.

The IR spectrum of HPEAQ shows a band at 1618 cm^{-1} for –N=CH– stretching vibrations [41,42]. After chelation with copper ions, this band shifted to a lower wavenumber. The frequency ν(C-O) and ν(C=O) bands appeared at 1243 and 1603 cm^{-1}, respectively, were shifted towards the lower sides

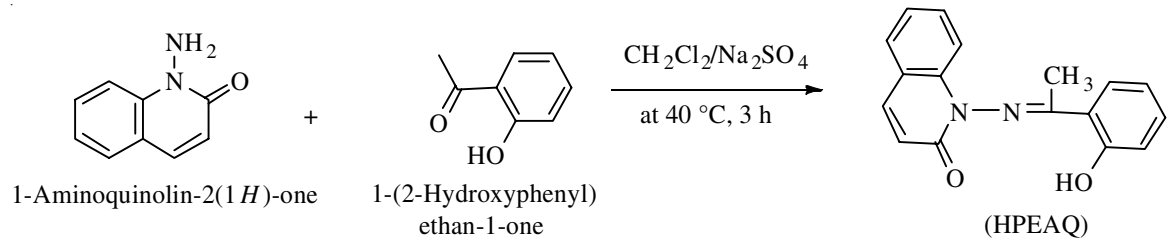

1-Aminoquinolin-2(1*H*)-one | 1-(2-Hydroxyphenyl) ethan-1-one | (HPEAQ)

Scheme-I: Preparation of HPEAQ

in Cu(II) hybrids, which indicated coordination through C–O and C=O, respectively (Fig. 1a). The -OH stretching vibration band appeared at 3055 cm^{-1} region [43] was disappeared after the chelation with copper ions. In $[Cu(HPEAQ)(H_2O)_2]$ spectra, the bands for Cu-O, Cu-N and Cu-Cl stretching vibrations appeared near 483-472, 543-538 and 349-334 cm^{-1}, respectively [44] (Fig. 1b).

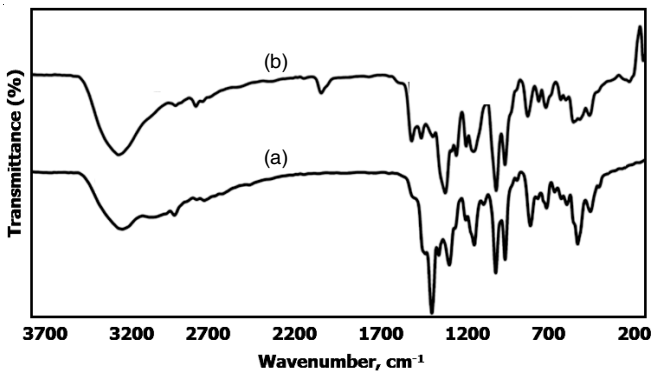

Fig. 1. IR spectra of HPEAQ (a) and Cu(II) hybrid **2** (b)

Mass analysis: The mass spectra of hybrid **2** and HPEAQ were also recorded. The *m/z* peaks corresponding to $[C_{16}H_{15}ClCuN_2O_4]^+$ and $[C_{17}H_{14}N_2O_2]^+$ ions were observed at 412 and 278, respectively (Fig. 2).

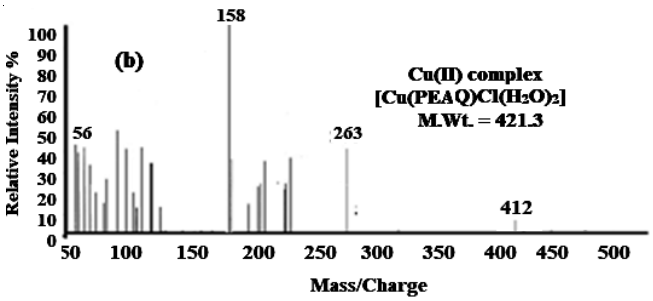

Fig. 2. Mass spectra of (a) HPEAQ and (b) Cu(II) hybrid **2**

Magnetic moment and UV-visible analysis of Cu(II) hybrid: The electronic spectra of HEPAQ (Fig. 3a) exhibited six bands due to π→π* and n→π* transitions in the UV region at 233, 274, 292, 338, 412 and 432 nm. The magnetic moment of nanocopper hybrid (**2**) was determined at 1.92 B.M. The electronic spectra of $[Cu(PEAQ)Cl(H_2O)_2]$ (Fig. 3b) presents the bands at 13,468, 19,146 and 26,762 cm^{-1} corresponding to $^2B_{1g}\rightarrow{}^2A_{1g}$ ($d_{x^2-y^2}\rightarrow d_{xy}$), $^2B_{1g}\rightarrow{}^2A_{1g}$ ($d_{x^2-y^2}\rightarrow d_{z^2}$), and $^2B_{1g}\rightarrow{}^2E_g$ ($d_{x^2-y^2}\rightarrow d_{xz}$, d_{yz}) transitions, respectively [45,46]. According to the aforementioned data, the molecular structure of the copper hybrid is assigned to be octahedral.

Thermal analysis: Thermogravimetry analysis/differential thermal analysis curves of Cu(II) hybrid (**2**) were obtained in 20-1000 ºC and indicated three weight loss steps at 140-210, 350-415 and 600-910 ºC (Fig. 4), which corresponded to coordinated water molecules. Primary weight loss was detected at 140-210 ºC caused by nanosized Cu(II) hybrid (**2**), which is in accordance with coordinated water molecules, HPEAQ moieties and CuO formation [47].

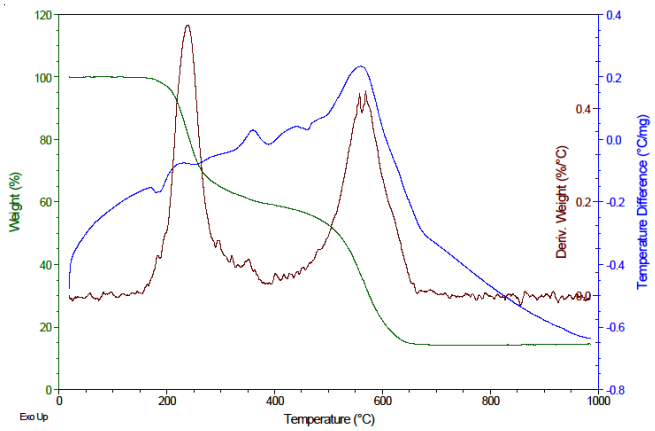

Fig. 4. TG-DTA traces of Cu(II) hybrid (**2**)

EPR spectra: According to the simulated and experimental EPR spectra of nanosized Cu(II) hybrid (**2**) (Fig. 5), the unpaired electron is present on the d_{z^2} elongated octahedral orbital in both the EPRs, in which $g_{\perp}$, g_{av}, $g_{\parallel}$ and $A_{\parallel}$ were observed at 2.04, 2.102, 2.21 and 12.3 Mt, respectively [48]. Orthorhombic g molecule parameters are supposed for octahedral geometries with a coordination number of six.

PXRD and SEM analysis: The powder X-ray diffraction (XRD) of nanosized Cu(II) hybrid (**2**) and the ligand HPEAQ

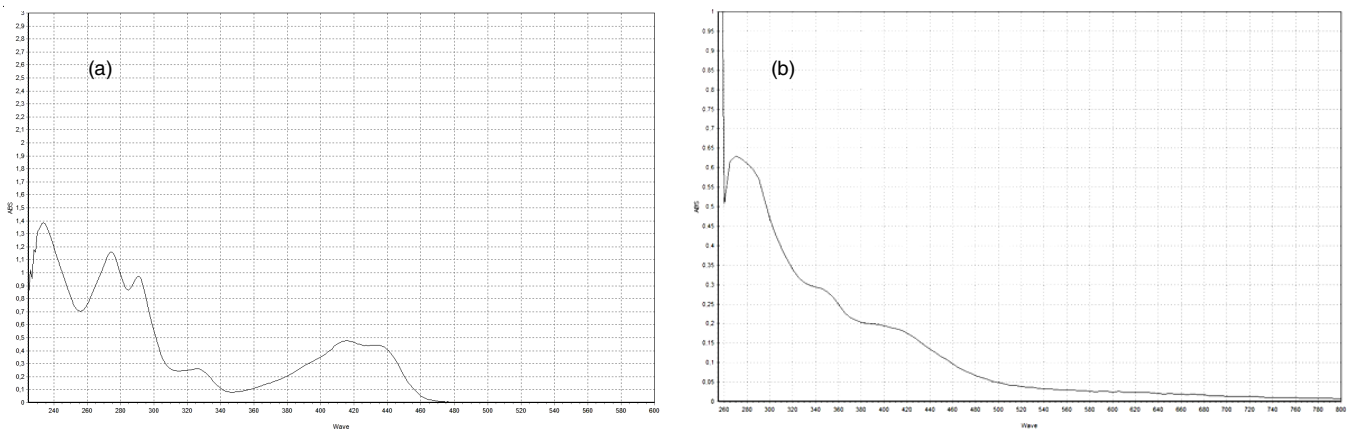

Fig. 3. Electronic spectra of (a) HPEAQ and (b) Cu(II) hybrid **2**

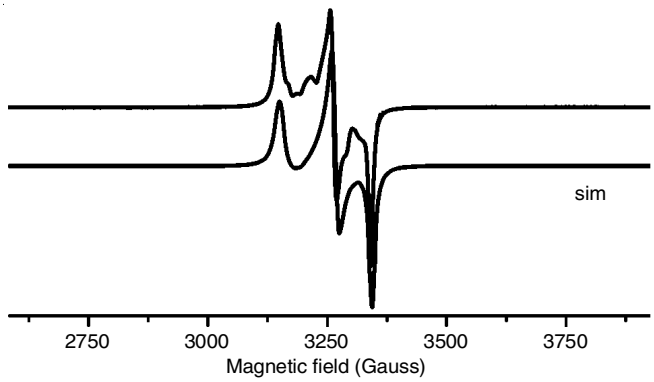

Fig. 5. EPR spectra of Cu(II) hybrid **2** in experimental and simulated

showed medium and sharp peaks, suggesting a crystalline nature (Fig. 6). Hybrid **2** shows novel peaks, indicating chelation of HPEAQ with copper ions. According to Scherrer's equation ($D = 0.9\ \lambda/\beta\cos\theta$) for Cu(II) hybrid, the crystal size is 42 nm. The particle size of hybrid **2** was determined using the SEM technique. This size was 10 μm and the shape was similar to broken ice pieces (Fig. 7). This value indicated a homogeneous matrix having the ideal shape of a material of uniform phase in nanosized Cu(II) hybrid **(2)**.

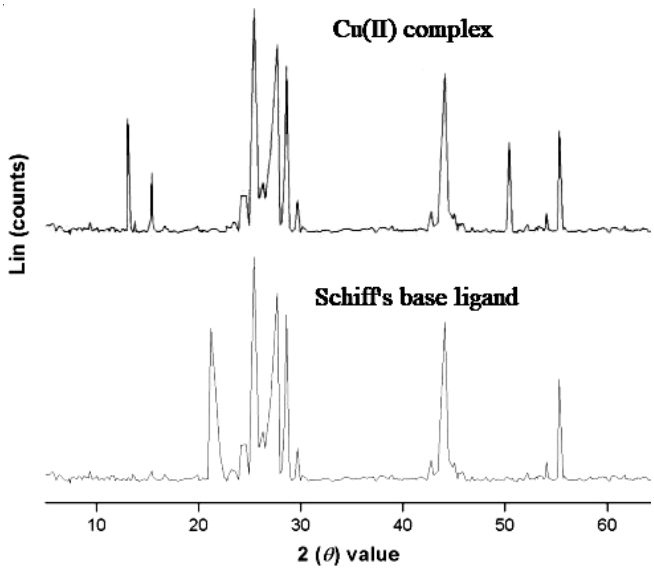

Fig. 6. PXRD pattern of HPEAQ and its nano-sized Cu(II) hybrid (**2**)

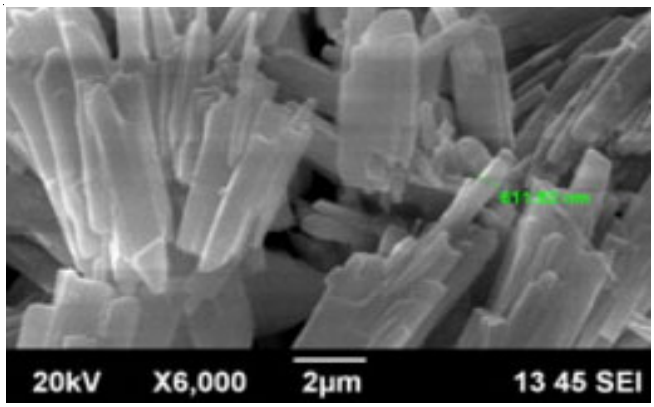

Fig. 7. SEM photograph of nano-sized Cu(II) hybrid (**2**)

DPPH free radical scavenging activity: The synthesized ligand HPEAQ and nanosized Cu(II) hybrid (**2**) have the highest ascorbic acid equivalent antioxidant capacity (AEAC). However, HPEAQ and nanosized Cu(II) hybrid (**2**) have the lowest corresponding IC_{50} of 1.82 and 0.663 mg/mL, respectively. The erythrocyte hemolysis and antioxidant activity of nanosized Cu(II) hybrid **(2)** and HPEAQ were analyzed using the ABTS assay (Tables 1 and 2). Nanosized hybrid **(2)** exhibits a strong antioxidant activity followed by HPEAQ.

TABLE-1
ABTS ANTIOXIDANT FOR HPEAQ AND NANO-SIZED Cu(II) HYBRID (**2**)

Compound	Absorbance	ABTS inhibition (%)
Control of ABTS	0.634	0
L-ascorbic acid	0.027	96.68
HPEAQ	0.359	35.84
Cu(II) hybrid	0.162	69.63

TABLE-2
ERYTHROCYTE HEMOLYSIS (%) OF FOR L HPEAQ AND NANO-SIZED Cu(II) HYBRID (**2**)

Compound	Absorbance	Erythrocyte hemolysis (%)
Distilled water	0.724	100
L-ascorbic acid	0.035	5.85
HPEAQ	0.042	6.44
Cu(II) hybrid	0.049	8.26

Antitumor activity using Ehrlich assay: An antitumor activity was identified in the synthesized ligand HPEAQ and nanosized hybrid (**2**). The results indicated that a higher cytotoxic activity was observed in HPEAQ (64.49%) than in nanosized Cu(II) hybrid (64.68%). Table-3 presents the variations in the percentage inhibition of the Ehrlich assays of the HPEAQ and nanosized copper(II) hybrid (**2**).

TABLE-3
EHRLICH INHIBITION % AT VARIOUS CONCENTRATIONS FOR HPEAQ AND NANO-SIZED Cu(II) HYBRID (**2**)

Compound	Concentration	Inhibition (%)
5-FU	0	40.23
	25	59.87
	100	93.62
HPEAQ	0	38.15
	25	54.29
	100	91.74
Cu(II) hybrid	0	32.56
	25	51.78
	100	89.73

Molecular docking studies with DNA and BSA: The conformation of docked nanosized Cu(II) hybrid **(2)** was also determined. The chelation of nanosized Cu(II) hybrid **(2)** was estimated using docking scores (Table-4), while the docking poses of nanosized Cu(II) hybrid (**2**) with EFGR kinase enzyme (1M17) and human LDHA receptor (4QT0) are shown in Fig 8 and 9, respectively.

TABLE-4
DOCKING RESULTS OF Cu(II) HYBRID WITH B-DNA, BSA PROTEIN, EGFR ENZYME AND HUMAN LDHA (kcal/mol)

	Binding energy ($\Delta G_{binding}$)	Vdw_hb_desolv energy ($\Delta G_{vdW+hb+desolv}$)	Electrostatic energy (ΔG_{elec})	Total internal energy (ΔG_{total})	Torsional free energy (ΔG_{tor})	Unbound system's energy (ΔG_{unb})
			B-DNA			
Hybrid	–12.5	–8.23	–0.98	–2.62	0.95	–1.62
			BSA protein			
Hybrid	–10.8	–7.17	–0.95	–2.08	0.92	–1.52
			EGFR enzyme			
Hybrid	–10.5	–7.15	–0.93	–2.01	0.89	–1.30
			Human LDHA			
Hybrid	–10.2	–6.87	–0.85	–1.92	0.82	–1.38

$\Delta G_{binding} = \Delta G_{vdW+hb+desolv} + \Delta G_{elec} + \Delta G_{total} + \Delta G_{tor} - \Delta G_{unb}$.

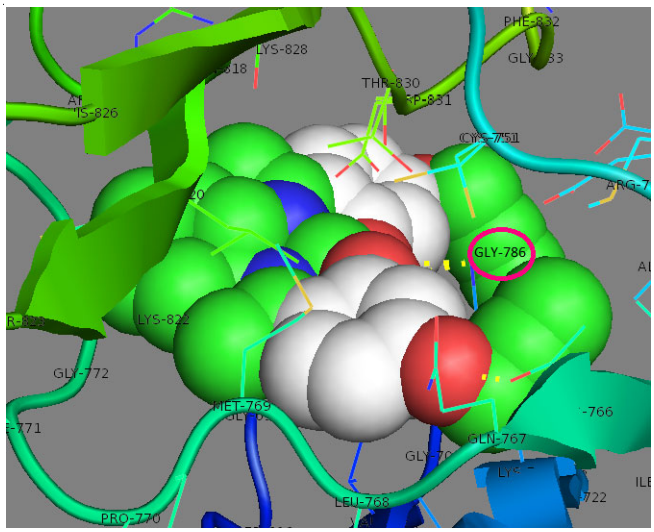

Fig. 8. Docking poses of nanosized Cu(II) hybrid (**2**) with EFGR kinase enzyme (1M17)

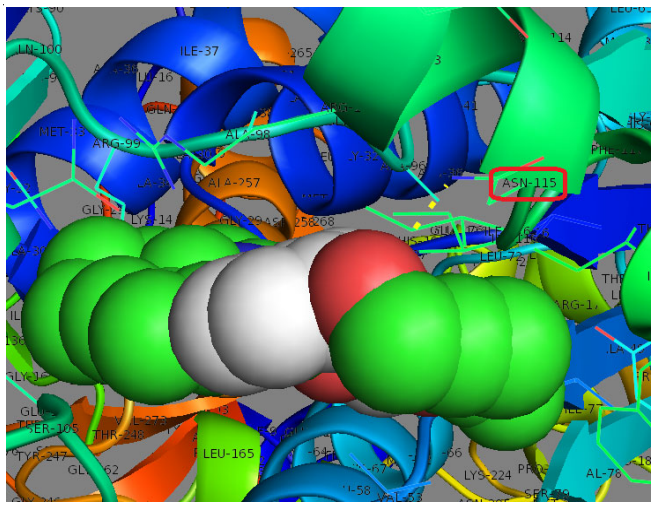

Fig. 9. Docking poses of nanosized Cu(II) hybrid with human LDHA receptor (4QT0).

Conclusion

Nanosized copper hybrids were successfully prepared using a simple hydrothermal route. The SEM and XRD results indicated that nanosized copper hybrids are observational. Temperature changes 120, 140 and 160 °C indicate a strong effect of hybrids on the morphology of nanocopper hybrids. The spectroscopy results and analytical data supports the octahedral geometry of the new prepared nanosized copper(II) hybrids (Fig. 10). The docking and biological studies of nanosized copper(II) hybrid (**2**) and the newly synthesized azomethine Schiff base ligand (2-hydroxyphenylethylideneamino)quinolin-2(1*H*)-one (HPEAQ) were also carried out.

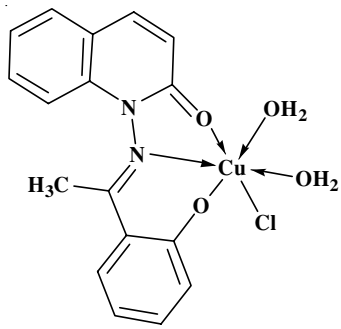

Fig. 10. Schematic representation of the Cu(II) hybrid

ACKNOWLEDGEMENTS

This work was funded by the Deanship of Scientific Research at Princess Nourah bint Abdulrahman University, Riyadh, Saudi Arabia, through the Research Groups Program Grant No. RGP-1440-0011.

CONFLICT OF INTEREST

The authors declare that there is no conflict of interests regarding the publication of this article.

REFERENCES

1. M.J. O'Donnell, *Acc. Chem. Res.*, **37**, 506 (2004); https://doi.org/10.1021/ar0300625
2. X. Ye, Y. Chen, C. Ling, R. Ding, X. Wang, X. Zhang and S. Chen, *Dalton Trans.*, **47**, 10915 (2018); https://doi.org/10.1039/C8DT02278J
3. S.Y. Ding, J. Gao, Q. Wang, Y. Zhang, W.G. Song, C.Y. Su and W. Wang, *J. Am. Chem. Soc.*, **133**, 19816 (2011); https://doi.org/10.1021/ja206846p
4. Z.A. De los Santos, R.S. Ding and C. Wolf, *Org. Biomol. Chem.*, **14**, 1934 (2016); https://doi.org/10.1039/C5OB02529J

5. N. Mohan, S.S. Sreejith, P.M.S. Begum and M.R.P. Kurup, *New J. Chem.*, **42**, 13114 (2018); https://doi.org/10.1039/C8NJ02657B
6. Y. Fu, Y. Tu, C. Fan, C. Zheng, G. Liu and S. Pu, *New J. Chem.*, **40**, 8579 (2016); https://doi.org/10.1039/C6NJ01458E
7. A.B. Pradhan, S.K. Mandal, S. Banerjee, A. Mukherjee, S. Das, A.R. Khuda Bukhsh and A. Saha, *Polyhedron*, **94**, 75 (2015); https://doi.org/10.1016/j.poly.2015.04.005
8. D.S. Ahmed, G.A. El-Hiti, A.S. Hameed, E. Yousif and A. Ahmed, *Molecules*, **22**, 1506 (2017); https://doi.org/10.3390/molecules22091506
9. Y. Liu, L. Mao, S. Yang, M. Liu, H. Huang, Y. Wen, F. Deng, Y. Li, X. Zhang and Y. Wei, *Dyes Pigments*, **158**, 79 (2018); https://doi.org/10.1016/j.dyepig.2018.05.032
10. D. Senol, *Hacettepe J. Biol. Chem.*, **45**, 67 (2017); https://doi.org/10.15671/HJBC.2017.142
11. H.-W. Ou, K.-H. Lo, W.-T. Du, W.-Y. Lu, W.-J. Chuang, B.-H. Huang, H.-Y. Chen and C.-C. Lin, *Inorg. Chem.*, **55**, 1423 (2016); https://doi.org/10.1021/acs.inorgchem.5b02043
12. F. Giordanetto, C. Tyrchan and J. Ulander, *ACS Med. Chem. Lett.*, **8**, 139 (2017); https://doi.org/10.1021/acsmedchemlett.7b00002
13. Y. Jia and J. Li, *Chem. Rev.*, **115**, 1597 (2015); https://doi.org/10.1021/cr400559g
14. J.L. Segura, M.J. Mancheño and F. Zamora, *Chem. Soc. Rev.*, **45**, 5635 (2016); https://doi.org/10.1039/C5CS00878F
15. P.A. Vigato and S. Tamburini, *Coord. Chem. Rev.*, **248**, 1717 (2004); https://doi.org/10.1016/j.cct.2003.09.003
16. R.M. Clarke, K. Herasymchuk and T. Storr, *Coord. Chem. Rev.*, **352**, 67 (2017); https://doi.org/10.1016/j.ccr.2017.08.019
17. T.J. Boyle, J.M. Sears, J.A. Greathouse, D. Perales, R. Cramer, O. Staples, A.L. Rheingold, E.N. Coker, T.M. Roper and R.A. Kemp, *Inorg. Chem.*, **57**, 2402 (2018); https://doi.org/10.1021/acs.inorgchem.7b01350
18. W. Al Zoubi and Y.G. Ko, *J. Organometal. Chem.*, **822**, 173 (2016); https://doi.org/10.1016/j.jorganchem.2016.08.023
19. P. Alreja and N. Kaur, *Inorg. Chim. Acta*, **480**, 127 (2018); https://doi.org/10.1016/j.ica.2018.05.010
20. C.M. da Silva, D.L. da Silva, L.V. Modolo, R.B. Alves, M.A. de Resende, C.V.B. Martins and A. de Fatima, *J. Adv. Res.*, **2**, 1 (2011); https://doi.org/10.1016/j.jare.2010.05.004
21. T.J. Boyle, D. Perales, J.M. Rimsza, T.M. Alam, D.M. Boye, J.M. Sears, J.A. Greathouse and R.A. Kemp, *Dalton Trans.*, **47**, 4162 (2018); https://doi.org/10.1039/C7DT04121G
22. A. Erxleben, *Inorg. Chim. Acta*, **472**, 40 (2018); https://doi.org/10.1016/j.ica.2017.06.060
23. M.T. Kaczmarek, M. Zabiszak, M. Nowak and R. Jastrzab, *Coord. Chem. Rev.*, **370**, 42 (2018); https://doi.org/10.1016/j.ccr.2018.05.012
24. A. Combes, *C.R. Acad. Sci. Fr.*, **108**, 1252 (1889).
25. R.J. Holbrook, D.J. Weinberg, M.D. Peterson, E.A. Weiss and T.J. Meade, *J. Am. Chem. Soc.*, **137**, 3379 (2015); https://doi.org/10.1021/jacs.5b00342
26. M. Hajrezaie, M. Paydar, S.Z. Moghadamtousi, P. Hassandarvish, C.Y. Looi, M.S. Salga, H. Karimian, K. Shams, M. Zahedifard, N.A. Majid, H.M. Ali and M.A. Abdulla, *Sci. Rep.*, **5**, 9097 (2015); https://doi.org/10.1038/srep09097
27. A. Hematpoor, M. Paydar, S.Y. Liew, Y. Sivasothy, N. Mohebali, C.Y. Looi, W.F. Wong, M.S. Azirun and K. Awang, *Chem. Biol. Interact.*, **279**, 210 (2018); https://doi.org/10.1016/j.cbi.2017.11.014
28. M. Zahedifard, F. Lafta Faraj, M. Paydar, C. Yeng Looi, M. Hajrezaei, M. Hasanpourghadi, B. Kamalidehghan, N. Abdul Majid, H. Mohd Ali and M. Ameen Abdulla, *Sci. Rep.*, **5**, 11544 (2015); https://doi.org/10.1038/srep11544
29. Â. de Fátima, C.P. Pereira, C.R.S.D.G. Olímpio, B.G. de Freitas Oliveira, L.L. Franco and P.H.C. da Silva, *J. Adv. Res.*, **13**, 113 (2018); https://doi.org/10.1016/j.jare.2018.03.007
30. S. Di Bella, A. Colombo, C. Dragonetti, S. Righetto and D. Roberto, *Inorg.*, **6**, 133 (2018); https://doi.org/10.3390/inorganics6040133
31. Z. Li, H. Yan, G. Chang, M. Hong, J. Dou and M. Niu, *J. Photochem. Photobiol. B*, **163**, 403 (2016); https://doi.org/10.1016/j.jphotobiol.2016.09.005
32. S. Mondal, M. Chakraborty, A. Mondal, B. Pakhira, A.J. Blake, E. Sinn and S.K. Chattopadhyay, *New J. Chem.*, **42**, 9588 (2018); https://doi.org/10.1039/C8NJ00418H
33. H.-Y. Yin, J. Tang and J.-L. Zhang, *Eur. J. Inorg. Chem.*, 5085 (2017); https://doi.org/10.1002/ejic.201700695
34. A. Enríquez-Cabrera, A. Vega-Peñaloza, V. Álvarez-Venicio, M. Romero-Ávila, P.G. Lacroix, G. Ramos-Ortiz, R. Santillan and N. Farfán, *J. Organomet. Chem.*, **855**, 51 (2018); https://doi.org/10.1016/j.jorganchem.2017.12.014
35. S. Ramezani, M. Pordel and A. Davoodnia, *Inorg. Chim. Acta*, **484**, 450 (2019); https://doi.org/10.1016/j.ica.2018.09.050
36. M. Burits and F. Bucar, *Phytother. Res.*, **14**, 323 (2000); https://doi.org/10.1002/1099-1573(200008)14:5<323::AID-PTR621>3.0.CO;2-Q
37. E.A. Lissi, B. Modak, R. Torres, J. Escobar and A. Urzua, *Free Radic. Res.*, **30**, 471 (1999); https://doi.org/10.1080/10715769900300511
38. A. El-Gazzar, M. Youssef, A. Youssef, A. Abu-Hashem and F. Badria, *Eur. J. Med. Chem.*, **44**, 609 (2009); https://doi.org/10.1016/j.ejmech.2008.03.022
39. Y. Morimoto, K. Tanaka, Y. Iwakiri, S. Tokuhiro, S. Fukushima and Y. Takeuchi, *Biol. Pharm. Bull.*, **18**, 1417 (1995); https://doi.org/10.1248/bpb.18.1417
40. I. Dhamija, N. Kumar, S. Manjula, V. Parihar, M.M. Setty and K. Pai, *Exp. Toxicol. Pathol.*, **65**, 235 (2013); https://doi.org/10.1016/j.etp.2011.08.009
41. J.R. Ferraro, Low-Frequency Vibrations of Inorganic and Coordination Compounds, Plenum Press: New York, p. 308 (1971).
42. K. Nakamoto, Infrared Spectra of Inorganic and Coordination Compounds, Part B, Wiley Interscience: New York, edn 5, p. 289 (1971).
43. S. Roy, T.N. Mandal, K. Das, R.J. Butcher, A.L. Rheingold and S.K. Kar, *J. Coord. Chem.*, **63**, 2146 (2010); https://doi.org/10.1080/00958972.2010.499457
44. P.P. Dholakiya and M.N. Patel, *Synth. React. Inorg. Met.-Org. Chem.*, **34**, 553 (2004); https://doi.org/10.1081/SIM-120030440
45. S. Chandra, Ruchi, K. Qanungo and S.K. Sharma, *Spectrochim. Acta Mol. Biomol. Spectrosc.*, **79**, 1326 (2011); https://doi.org/10.1016/j.saa.2011.04.063
46. A.K. Sharma and S. Chandra, *Spectrochim. Acta A Mol. Biomol. Spectrosc.*, **81**, 424 (2011); https://doi.org/10.1016/j.saa.2011.06.032
47. C. Duval, Inorganic Thermogravimetric Analysis, Elsevier, Amsterdam, edn 2, p. 243 (1963).
48. G. Plesch, C. Friebel, O. Švajlenová and J. Krätsmár-Šmogroviè, *Polyhedron*, **14**, 1185 (1995); https://doi.org/10.1016/0277-5387(94)00377-Q